The three roots, m_1, m_2, m_3 are shown as functions of ν in Fig. 1. It is notable that the second root, m_2, is very close to the function $1/\Lambda$, when ν is small. In fact, it can be shown that

$$m_2 = \frac{1}{\Lambda} + 32\epsilon^4 + O(\epsilon^5) \tag{30}$$

for $\nu \ll 1$, where

$$\epsilon = \frac{1}{2} - \Lambda = \frac{\nu}{2(1-\nu)}. \tag{31}$$

We also note that the results permit the left-hand side of (3) to be factorized explicitly in the form $(m - m_1)(m - m_2)(m - m_3)$. It follows that the function $R(V)^{-1}$, which appears in Lamb's solution (1904) for an impulsive load and Cole and Huth's solution (1985) for a moving line load, can be written in the rationalized form

$$\frac{1}{R(V)} = \frac{(2 - M_2^2)^2 + 4\sqrt{(1 - M_1^2)(1 - M_2^2)}}{M_2^2(M_2^2 - m_1)(M_2^2 - m_2)(M_2^2 - m_3)} \tag{32}$$

which can be expanded as a set of partial fractions if desired.

Acknowledgments

J. R. Barber is pleased to acknowledge support from the National Science Foundation under Contract No. MSS-9200762.

References

Achenbach, J. D., 1984, *Wave Propagation in Elastic Solids*, Elsevier, New York.

Aki, K., and Richards, P. G., 1980, *Quantitative Seismology: Theory and Methods*, Vol. I, Freeman, San Francisco, CA.

Auld, B. A., 1973, *Acoustic Fields and Waves in Solids*, Vol. I and Vol. II, John Wiley and Sons, New York.

Ben Menahem, A., and Singh, S. J., 1981, *Seismic Waves and Sources*, Springer-Verlag, New York.

Brekhovskikh, L. M., and Godin, O. A., 1990, *Acoustics of Layered Media: Plane and Quasi-plane Waves*, Vol. I, Springer-Verlag, Berlin, Germany.

Bullen, K. E., 1963, *An Introduction to Theory of Seismology*, Cambridge University Press, Cambridge, U.K.

Cagniard, L., 1964, *Reflection and Refraction of Progressive Seismic Waves*, McGraw-Hill, New York.

Cole, J. D., and Huth, J. H., 1958, "Stresses Produced in a Half-Plane by Moving Loads," ASME JOURNAL OF APPLIED MECHANICS, Vol. 25, pp. 433–436.

Cowles, W. H., and Thompson, J. E., 1947, *Algebra*, D. Van Nostrand Company, New York.

Eringen, A. C., and Suhubi, E. S., 1975, *Elastodynamics: Linear Theory*, Vol. 2, Academic Press, New York.

Ewing, W. M., Jardetzky, W. S., and Press, F., 1957, *Elastic Waves in Layered Media*, McGraw-Hill, New York.

Fedorov, F. I., 1968, *Theory of Elastic Waves in Crystals*, Plenum Press, New York.

Hanyga, A., ed., 1985, *Seismic Wave Propagation in the Earth*, Elsevier-PWN, Amsterdam.

Hayes, M., and Rivlin, R. S., 1962, "A Note on the Secular Equation for Rayleigh Waves," *ZAMP*, Vol. 13, pp. 80–83.

Jeffreys, H., 1952, *The Earth*, Cambridge University Press, Cambridge, U.K.

Kolsky, H., 1963, *Stress Waves in Solids*, Dover, New York.

Lamb, H., 1904, "On the Propagation of Tremors over the Surface of an Elastic Solid," *Phil. Trans. Royal Soc., London*, Vol. A203, pp. 1–42.

Love, A. E. H., 1944, *A Treatise on the Mathematical Theory of Elasticity*, 4th ed., Dover, New York.

Mal, A. K., and Singh, S. J., 1991, *Deformation of Elastic Solids*, Prentice-Hall, Englewood Cliffs, NJ.

Viktorov, I. A., 1967, *Rayleigh and Lamb Waves*, Plenum Press, New York.

Critical Strain Ranking of 12 Materials in Deformations Involving Adiabatic Shear Bands

R. C. Batra[22,25], X. Zhang[23], and T. W. Wright[24,25]

Batra and Kim (1992) studied the initiation and growth of shear bands in 12 materials deformed in simple shear. Each material was modeled by the Johnson-Cook (1983) law, values of material parameters were taken from Johnson and Cook's (1983) paper, and the effects of inertia forces and thermal conductivity were included. However, materials generally are rarely tested in simple shear and the material data used was derived from tests conducted over a moderate range of strains, strain rates, and temperatures. In this Note, we report results of numerical simulation of torsion tests similar to those performed by Marchand and Duffy (1988) on HY-100 steel and rank 12 materials according to the values of the nominal strain at which the torque begins to drop precipitously. Values of material parameters taken from Rajendran's report (1992) and likely to be valid over a large range of strains, strain rates, and temperatures are used. However, the effect of thermal conductivity has been neglected because the computer code DYNA3D (Whirley and Hallquist, 1991) employed to study the problem assumes locally adiabatic deformations. Batra and Kim (1991) have shown that for simple shearing deformations of viscoplastic materials, realistic values of thermal conductivity have little effect on the values of the nominal strain at which deformations begin to localize and thus shear bands initiate.

In the simulations reported herein, the initial thickness, $\omega(z)$, of the tube with inner radius of 4.75 mm is assumed to vary according to the relation

$$\omega(z) = 0.19\left[1.9 + 0.1\sin\left(\frac{1}{2} + \frac{2z}{2.5}\right)\pi\right]\text{mm}, \quad 0 \le z \equiv 2.5\text{ mm}. \tag{1}$$

Here z denotes the position of a point along the axis of the tube with $z = 0$ being the fixed end. The end $z = 2.5$ mm is twisted so as to produce a nominal strain rate of 5000 s^{-1}. It is assumed that the angular speed increases from zero to the steady value of 2530 rad/s in 20 μs. The thickness variation, depicted in Fig. 1, clearly shows that the minimum tube thickness occurs at its center, and equals 90 percent of that at its outer edges.

The tube is assumed to be initially at rest, stress-free, and at the room temperature, T_o, of 25°C. The inner and outer surfaces of the tube are taken to be traction-free and thermally insulated, and its deformations are assumed to be

[22] Department of Engineering Science and Mechanics, Virginia Polytechnic Institute and State University, Blacksburg, VA 24061–0219.

[23] 144 Yorkshire Boulevard, No. 206, Dearborn Heights, MI 48127.

[24] U.S. Army Research Laboratory, Aberdeen Proving Ground, MD 21005-5066.

[25] Fellow ASME.

Contributed by the Applied Mechanics Division of THE AMERICAN SOCIETY OF MECHANICAL ENGINEERS for publication in the ASME JOURNAL OF APPLIED MECHANICS. Manuscript received by the ASME Applied Mechanics Division, Sept. 7, 1993; final revision, Feb. 18, 1994. Associate Technical Editor: W. N. Sharpe, Jr.

locally adiabatic. The thermomechanical response of each one of the 12 materials is modeled by the Johnson-Cook (1983) law:

$$\sigma_m = \left(A + B\gamma_p^n\right)\left(1 + C \ln \dot{\gamma}_p/\dot{\gamma}_o\right)\left(1 - T^{*m}\right);$$

$$T^* = \frac{(T - T_o)}{(T_m - T_o)}, \quad (2)$$

where σ_m is the equivalent or the effective stress, A equals the yield stress in a quasi-static simple tension or compression test, B and n characterize the strain hardening of the material, C characterizes its strain rate sensitivity, and the factor $(1 - T^{*m})$ determines the decrease in the flow stress because of the temperature rise. In Eq. (2) γ_p is the effective plastic strain, T_m the melting temperature of the material, and $\dot{\gamma}_o$ is the reference strain rate of 1/sec. Values of material parameters A, B, n, C, m, the mass density ρ, and the specific heat c are taken either from Rajendran (1992) or from a handbook, and are listed in Table 1. Values of the shear and bulk moduli are needed to account for the small elastic deformations of the tube material.

The transient thermomechanical problem is analyzed by using the large-scale explicit finite element code DYNA3D (Whirley and Hallquist, 1991) with a suitably graded finite element mesh consisting of 8-noded brick elements with 30 elements along the axial length of the tube, 4 elements across the thickness, and 40 elements along the circumference. In the axial direction, elements are finer near the center of the tube and increase in size gradually as one moves towards the ends of the tube. Preliminary computations indicated that the deformations of the tube were axisymmetric and stayed uniform through the thickness of the tube.

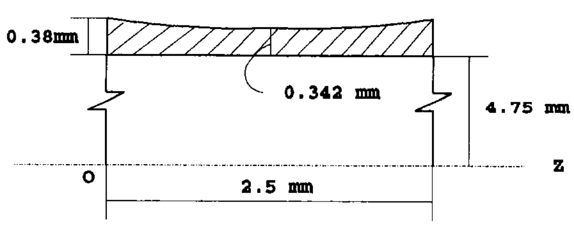

Fig. 1 The presumed variation in the thickness of the tube

Figures 2 and 3 depict the time history of the torque required to deform the tube and the evolution of the effective plastic strain at the tube center for the 12 materials studied. In each case, the torque initially increases because of the increase in the angular speed of the twisted end, and continues to increase because of the hardening of the mate-

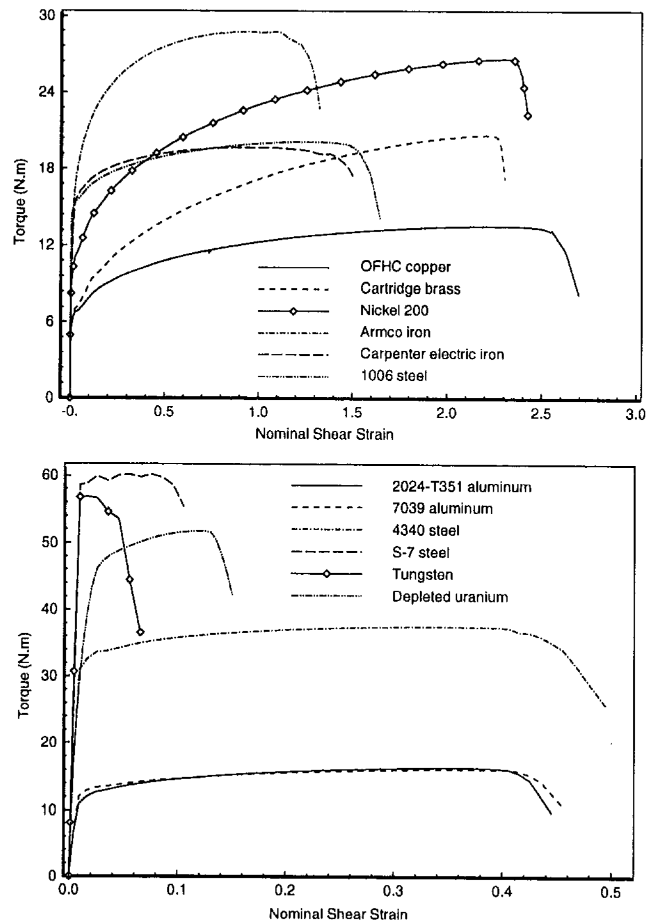

Fig. 2 The torque required to deform the tube versus the nominal shear strain

Table 1 Material constants for the Johnson-Cook model

Material	A MPa	B MPa	C	n	m	ρ kg/m³	θ_m °C	K GPa	μ GPa	c (J/kg°C)
OFHC Copper	89.63	291.64	0.025	0.31	1.09	8,960	1,083	138	42	383
Cartridge Brass	111.69	504.69	0.009	0.42	1.68	8,520	916	112	41	385
Nickel 200	163.40	648.10	0.006	0.33	1.44	8,900	1,453	198	80	446
Armco Iron	175.12	800.00	0.06	0.32	0.55	7,890	1,538	140	76	452
Carpenter Electric Iron	289.58	338.53	0.055	0.40	0.55	7,890	1,538	162	78	452
1006 Steel	350.25	275.00	0.022	0.36	1.00	7,890	1,538	169	80	452
2024-T351 Aluminum	264.75	426.09	0.015	0.34	1.00	2,770	502	76	28	875
7039 Aluminum	336.46	342.66	0.01	0.41	1.00	2,770	604	81	28	875
4340 Steel	792.19	509.51	0.014	0.26	1.03	7,840	1,520	157	76	477
S-7 Tool Steel	1538.89	476.42	0.012	0.18	1.00	7,750	1,490	246	117	477
Tungsten	1505.79	176.50	0.016	0.12	1.00	17,000	1,450	257	133	134
Depleted Uranium	1079.01	1119.69	0.007	0.25	1.00	18,600	1,200	92	58	117

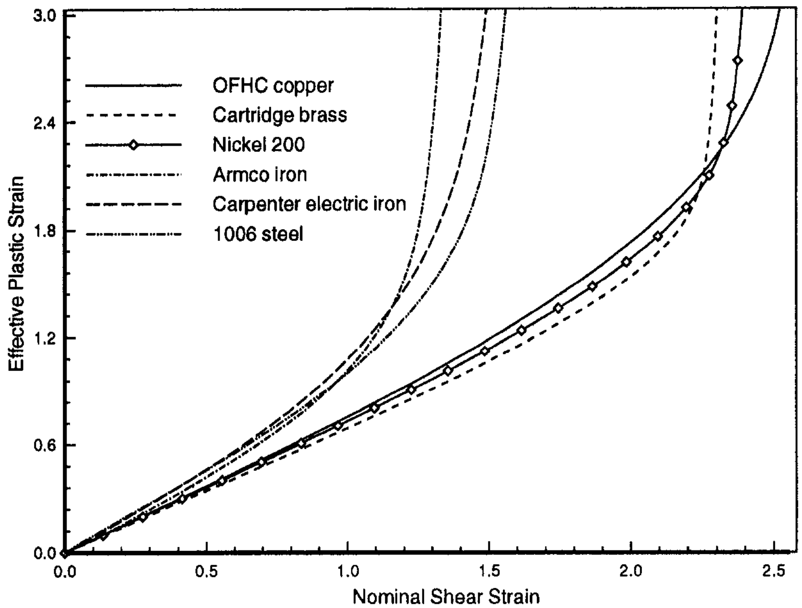

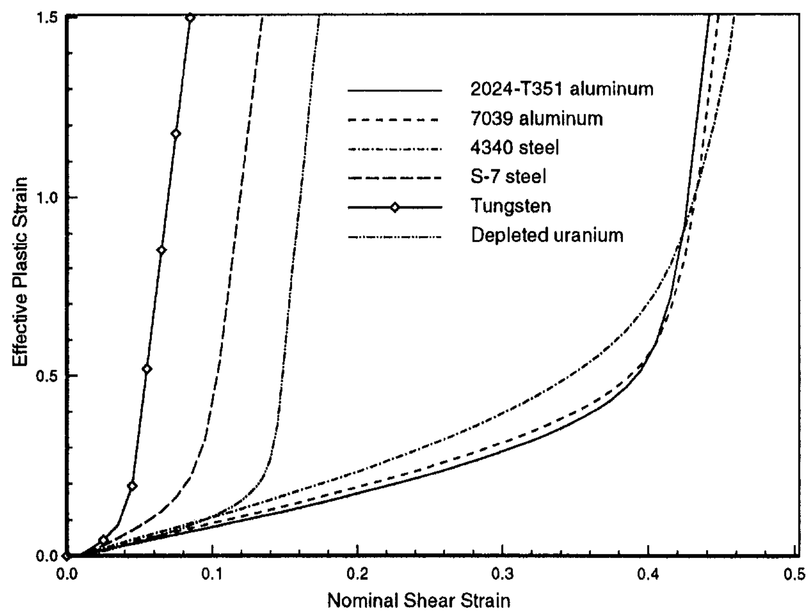

Fig. 3 The effective plastic strain at the band center versus the nominal shear strain

rial due to strain and strain rate effects. However, when thermal softening of the material at the tube center exceeds the hardening of material there, the torque required to deform the tube decreases. For each one of the 12 materials except one (Carpenter electric iron) studied herein, the torque drops precipitously prior to the slope of the torque versus nominal shear strain curve becoming zero. This is due to the rather high value of the assumed variation of the tube thickness. Computations done with five percent variation in the thickness for three materials, namely, OFHC copper, 4340 steel, and 2024-T351 aluminum, yielded similar results except that the slope of the curve representing the torque versus the nominal shear strain became zero prior to the rapid drop in the torque. For each material studied, the effective plastic strain at the tube center first gradually increases with an increase in the nominal strain, but when the torque begins to drop, the effective plastic strain at the tube center begins to increase sharply. We note that the deformations localized into essentially one element near the middle of the tube, and subsequently all of the deformations occurred only in this element. Computations were stopped shortly after this stage.

We presume that the shear band initiates when the torque drops quickly, which essentially coincides with the instant of rapid increase of the effective plastic strain at the tube center, and we rank materials according to the value of the nominal strain at which this occurs. Marchand and Duffy (1988), based on their experimental observations, pointed out that a shear band initiates when the shear stress begins to drop rapidly. In the twelve materials studied herein, shear bands initiate in the following order: Tungsten, S-7 tool steel, Depleted Uranium, 2024-T351 aluminum, 7039 aluminum, 4340 steel, Armco iron, Carpenter electric iron, 1006 steel, Cartridge brass, Nickel 200 and OFHC copper. Computations for the aforestated three materials with five percent thickness variation did not change their ranking as far as the nominal strain at the initiation of the shear band is concerned; this leads us to conclude that the amount of thickness variation does not affect the ranking. We note that the nominal strain when the torque drops rapidly depends upon the assumed variation in the tube thickness, and also upon the finite element mesh used. Besides the size and shape of the geometric defect, other factors such as the mass density, specific heat, thermal conductivity, the nominal strain rate, strain and strain-rate hardening effects, and the rate of thermal softening affect the value of the nominal strain at the instant of the initiation of a shear band; e.g., see Wright (1992). Batra and Kim (1992) used a very fine finite element mesh within and around the shear band region to study the effect of geometric defect size on the localization of deformations in simple shearing deformations of different materials. They found that the defect size had no effect on the critical strain ranking of the 12 materials studied. The results presented herein are intended to help an experimentalist answer the following question: Among the 12 materials studied herein, having found the nominal strain at which a shear band initiates in torsional tests in a material, at what value of the nominal strain will a shear band initiate in an identical tube made of a different material? Also, these results should help ascertain the validity of any future analytical results obtained on the value of the nominal strain at which a shear band initiates in a material.

Ballistic experiments (Magness and Farrand, 1990) with tungsten and depleted uranium penetrators and steel targets suggest that shear bands initiate first in uranium, in contradiction to the ranking obtained herein. In penetration tests, the state of stress around a penetrator nose is triaxial rather than that of simple shearing. The problem of the initiation of shear bands under such general states of stress has not been studied so far.

Acknowledgments

This work was partially supported by the U.S. Army Research Office grant DAAL03-91-G-0084 and the NSF grant MSS9121279 to the University of Missouri-Rolla. X. Zhang and R. C. Batra thank Dr. Robert G. Whirley of the Lawrence Livermore Laboratory, California, for his help with the DYNA3D code.

References

Batra, R. C., and Kim, C. H., 1992, "Analysis of Shear Banding in Twelve Materials," *International Journal of Plasticity*, Vol. 8, pp. 425–452.

Batra, R. C., and Kim, C. H., 1991, "Effect of Thermal Conductivity on the Initiation, Growth and Band Width of Adiabatic Shear Bands," *International Journal of Engineering Science*, Vol. 29, pp. 949–960.

Johnson, G. R., and Cook, W. H., 1983, "A Constitutive Model and Data for Metals Subjected to Large Strains, High Strain Rates, and High Temperatures," *Proceedings of 7th International Symposium Ballistics*, The Hague, The Netherlands, pp. 541–548.

Magness, L. S., and Farrand, T., 1990, "Deformation Behavior and its Relationship to the Penetration Performance of High-Density KE Penetrator Materials," *Proceedings of 1990 Army Science Conference*, West Point, NY.

Marchand, A., and Duffy, J., 1988, "An Experimental Study of the Formation Process of Adiabatic Shear Bands in a Structural Steel," *Journal of the Mechanics and Physics of Solids*, Vol. 36, pp. 251–283.

Rajendran, A. M., 1992, "High Strain Rate Behavior of Metals, Ceramics and Concrete," Report #WL-TR-92-4006, Wright Patterson Air Force Base.

Whirley, R. G., and Hallquist, J. O., 1991, "DYNA3D User's Manual (A Nonlinear, 'Explicit,' Three-Dimensional Finite Element Code for Solid and Structural Mechanics)," UCRL-MA-107254, Univ. of California, Lawrence Livermore National Laboratory.

Wright, T. W., 1992, "Shear Band Susceptibility: Work Hardening Materials," *International Journal of Plasticity*, Vol. 8, pp. 583–602.

Existence of Stoneley Waves at an Unbonded Interface Between Two Micropolar Elastic Half-Spaces

M. Tajuddin[26]

Following Eringen's theory, the question whether a Stoneley mode can exist at an unbonded interface between two micropolar elastic half-spaces is examined analytically. Explicit conditions for its existence are derived when the two half-spaces are incompressible or Poisson solids whose material properties are close to each other.

1 Introduction

It is merely not possible to apply just the classical theory to engineering problems related to oriented media like polycrystalline materials or materials with a fibrous or coarse-grained structure. The micropolar theory of elasticity describing the behavior of oriented materials is proposed by Eringen (1966).

In the present analysis an attempt is made to study the micropolar effect on the Stoneley wave propagation at an unbonded interface between two half-spaces based on Eringen's theory together with the method of Murty (1975). By considering the plane harmonic waves, the analysis yields two frequency equations. It is seen from the first frequency equation that the wave is propagating with an extra velocity, known as micropolar wave, which has no counterpart in classical theory. This may be attributed to the micropolar nature of the medium. The second frequency equation is the counterpart of the Stoneley wave equation of classical theory discussed when the two half-spaces are incompressible or when the Poisson solids, those material properties are close to each other, by using a power series method. Explicit conditions for its existence are derived. The results of classical theory are shown as a special case (Murty, 1975).

2 Solution of the Problem

Consider two micropolar elastic half-spaces whose unbonded interface constitutes a plane surface $z = 0$. A set of rectangular coordinate axes is chosen with the origin at the interface, the x-axis in the direction of propagation and the z-axis into the interior of the lower half-space. In such a case the displacement and microrotation vectors are, respectively, $(u, 0, w)$ and $(0, \phi, 0)$, which are functions of x, z, and time t. The functions u, w, and ϕ satisfy the equations of motion if

[26]Department of Mathematics, Nizam College (O.U.), Hyderbad 500 001 (A.P.), India.

Contributed by the Applied Mechanics Division of THE AMERICAN SOCIETY OF MECHANICAL ENGINEERS for publication in the ASME JOURNAL OF APPLIED MECHANICS. Manuscript received by the ASME Applied Mechanics Division, May 25, 1993; final revision, Dec. 20, 1993. Associate Technical Editor: R. M. Bowen.